LAWRENCE
LIVERMORE
NATIONAL
LABORATORY

LLNL-CONF-768704

Subsurface Monitoring via Physics-Informed Deep Neural Network Analysis of DAS

C. S. Sherman, R. J. Mellors, J. P. Morris

March 1, 2019

50th US Rock Mechanics Symposium / Geomechanics Symposium
New York, NY, United States
June 23, 2019 through June 26, 2019

Disclaimer

Subsurface Monitoring via Physics-Informed Deep Neural Network Analysis of DAS

Sherman, C.S., Mellors, R.J., and Morris, J.P.
Lawrence Livermore National Laboratory, Livermore, CA, USA
LLNL-CONF-768704

ABSTRACT: Fiber optic based distributed acoustic sensors (DAS) provide a new approach for monitoring signals of interest in the subsurface with unprecedented spatiotemporal resolution. These sensors produce measurements that are fundamentally different from their traditional counterparts, such as geophones, and produce significantly larger volumes of data. To interpret these data, we begin by using the physics-based thermal-hydraulic-mechanical (THM) model in the GEOS code to simulate synthetic DAS measurements for a range of subsurface conditions (fracture propagation, fault slip, etc.) and sensor configurations (e.g.: horizontal or vertical well deployments). These synthetic DAS measurements are then algorithmically labeled based upon features of interest within their parent models, such as the extent of any generated hydraulic fractures or the distribution of proppant particles, and are compiled into a database. The synthetic database can be used to train and test an initial deep neural network (DNN) representation of the subsurface, which can then be optimized by incorporating any available field measurements through transfer learning. This hybrid, physics informed DNN model is capable of interpreting DAS measurements in near-real time, making it a useful tool for decision making by field engineers, and works under both data-rich and data-poor conditions. To demonstrate this approach, we consider the problem of imaging hydraulic fracture propagation in an unconventional oil and gas reservoir. Our results indicate that we are can use a trained DNN model to accurately estimate the extents of a hydraulic fracture using the location information and DAS measurements for a single fiber-optic sensor as inputs.

1. INTRODUCTION

The development of fiber-optic distributed sensor technology provides an avenue for measuring signals of interest ranging from acoustic and seismic waves (DAS) to temperature (DTS). These sensors operate by sending a sequence of laser pulses down the fiber that interact with imperfections in the glass, backscatter towards the source, and are recorded by an interferometer. In the case of DAS, variations in the phase of the return signal are used to estimate the strain (or strain-rate) parallel to the fiber. These measurements occur at regular intervals (typically on the order of a meter) along the length of the fiber (up to several kilometers), and represent a spatial average over a gague length (typically 1 to 10 m) (Daley et al., 2013; Mateeva et al., 2014; Hartog, 2017). Because these sensors provide unparalleled resolution, are relatively inexpensive, an can be deployed inside or outside a well casing, they are often deployed to monitor subsurface processes. Low-frequency DAS measurements have been particularly useful for monitoring psuedostatic processes such as hydraulic fracturing (Hull et al., 2017; Jin and Roy, 2017; Karrenbach et al., 2017).

Because these sensors produce measurements that are fundamentally different from conventional geophysical sensors (e.g.: geophones), it is necessary to develop new strategies for processing and interpreting their data. Recent advances in machine learning (ML) provide an avenue for doing so in an efficient, data-driven manner. Because DAS provides an inherently two-dimensional measurement, advances in image-recognition using deep neural network (DNN) analysis (e.g.: Krizhevsky et al., 2012) are particularly relevant to this problem.

2. METHODOLOGY

Instead of simply re-purposing an existing network, the goal of this work is to develop a physics-informed framework to interpret DAS measurements and to monitor subsurface processes. To demonstrate this, we focus on the problem of monitoring the development of hydraulic fractures using low-frequency DAS. In the following, we discuss our numerical model of the subsurface, the datasets we use for training and testing, and the DNN design.

2.1. Numerical Model

A key component of a supervised ML analysis is *labeled* training data. While there are a large number of DAS measurements recorded during hydraulic stimulations available (data), direct measurements of fracture extent (labels) are rare. Instead of using field data, we use a method for modeling DAS using the 3D thermo-hydro-mechanical (THM) code GEOS (Sherman et al., 2018; Settgast et al., 2016).

To simulate DAS measurements, we construct models of the subsurface in which we generate a single, vertical hydraulic fracture. In each of these, we insert a set of virtual fiber-optic sensors throughout the model, oriented both vertically and

horizontally. After each stimulation, we algorithmically label each dataset with key observations: the position of the fiber with respect to the fracture (dx, dy, dz), the global height (H) and top (T) of the fracture, and the height (H_local) and top (T_local) of the fracture nearest to the sensor.

2.2. Dataset Design

To generate the necessary dataset for the ML analysis, we constructed 100 distinct hydraulic fracturing models, each with 136 virtual fiber-optic sensors. To generate a wide variety of fracture shapes and sizes, we draw the individual model parameters from a series of random-uniform distributions given in Table 1. A realization of the in-situ stress state and the pumping schedule for a model in database are shown in Figures 1 and 2. The base in-situ stress model assumes a uniform density through the model. Variations in the minimum horizontal stress (σ_h) are sampled from a random fractal distribution. Each hydraulic stimulation is designed in three stages (A, B, and C) with increasing fluid viscosity, a uniform flow rate, and proppant injection beginning in stage B.

Table 1: The distribution of parameters used to generate each hydraulic fracturing simulation.

Model Parameter	Min	Max
σ_h standard deviation (MPa)	1	2
σ_h fractal dimension	-0.25	0.25
Fluid injection rate (m^3/s)	0.0376	0.067
Fluid A injection time (min)	20	40
Fluid A viscosity (cP)	1	5
Fluid B injection time (min)	20	40
Fluid B viscosity (cP)	7.5	50
Fluid C injection time (min)	20	40
Fluid C viscosity (cP)	75	500
Proppant volume fraction	0.1	0.2

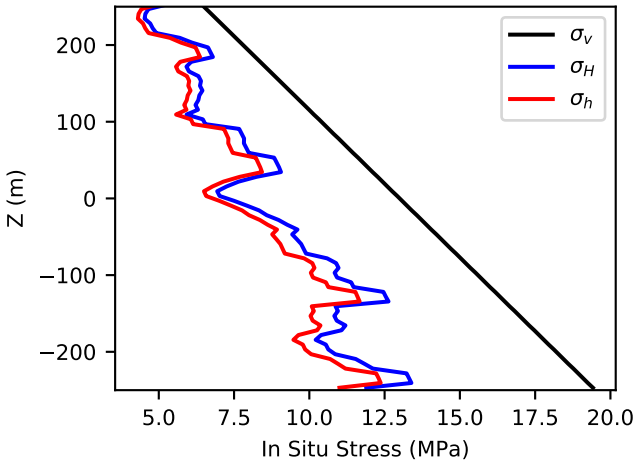

Figure 1: A realization of the in-situ stress state for a model in the database.

Approximately 500,000 cpu-core*hours were required to run all of the models in the dataset. As a post-processing step, each of the DAS measurements are scaled by their maximum values and are re-sampled into 124x496 pixel images. The units of the remaining data and labels are converted to pixels, and are scaled to conform to a standard normal distribution. Each of the entries in the dataset are then randomly assigned to either the model training (85%) or testing (15%) datasets. To enhance the training dataset, we add additional entries by considering model symmetry and by performing simple geometric transformations to the data and labels.

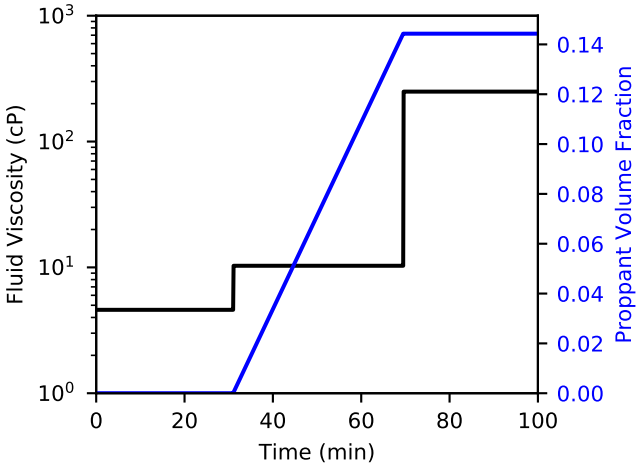

Figure 2: A realization of the fluid injection schedule for a model in the database.

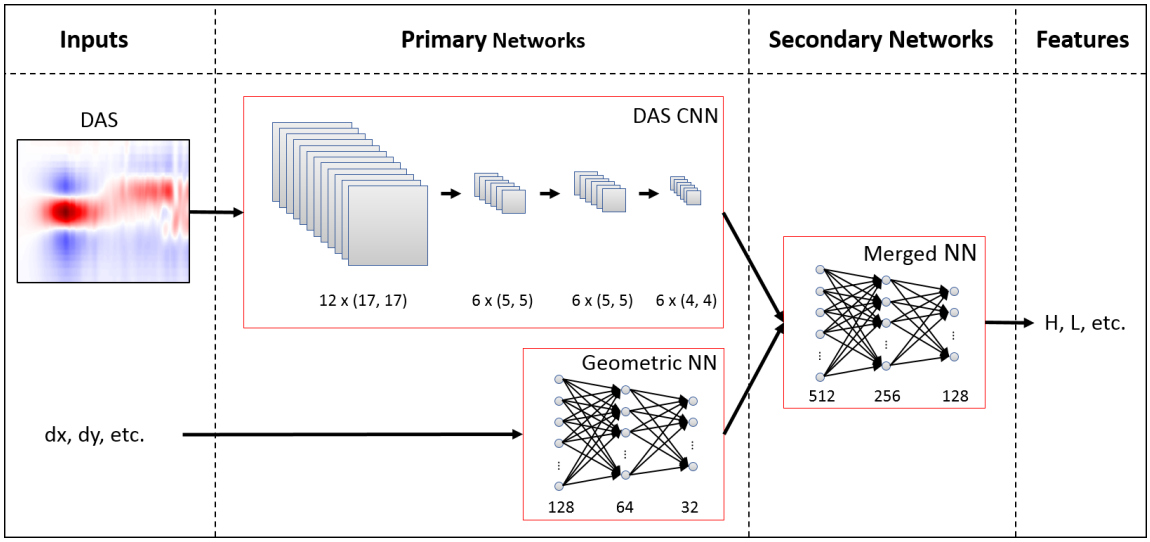

Figure 3: An overview of the DNN used to estimate the fracture extents from DAS measurements. The network is split into several sub-networks which use either convolutional or fully-connected neurons to process the data. The numbers beneath each sub-network indicate the size and number of neurons used in one realization of this model.

2.3. DNN Design

A significant advantage of using a DNN to interpret data over traditional methods is that they provide a natural framework for mapping arbitrary inputs to arbitrary outputs. For example, one of the most successful implementations of DNNs are image-classification networks, which take a series of M x N arrays for each color channel as input, and output a class label (Krizhevsky et al., 2012).

As part of our analysis, we designed and trained a group of DNNs to map the observed DAS measurements and known geometric quantities (the distance from the fiber-optic sensor to the target fracture) to an array of scalar values that describe the extents of the fracture (height, the top of the fracture, etc.). Because the DAS measurements are essentially monochrome images, we adopt some of the structures commonly found within image-recognition networks to process the data. Figure 3 gives an overview of the DNN topology, which is split into a series of sub-blocks:

- Input Layer - this is the entry point for the DNN. The top branch accepts the DAS measurements and the lower branch accepts the geometric parameters as inputs.
- DAS CNN - this block uses a series of convolutional layers to process the 2D DAS measurements. Batch-normalization and max-pooling layers are inserted between certain convolutional to improve training stability and avoid over-fitting.
- Geometric NN - this block uses a fully-connected neural network to process the geometric inputs. Similar to the DAS

CNN, dropout layers are inserted between certain layers to improve stability and avoid over-fitting.

- Merged NN - this block begins by flattening and concatenating the outputs of the DAS CNN and Geometric DNN into a single 1D vector. It then processes these values using a series of fully-connected and dropout layers.
- Feature Layer - this is where the the features of interest are calculated.

The network is implemented in Python using the Keras module (Chollet, 2015) and the Tensoflow backend (Abadi et al., 2015). We used the adam gradient-descent algorithm to train the network, with a momentum equal to 0.9 and epsilon equal to 1e-6. With the exception of the feature layer, which used a linear activation function, each of the neurons in the network used a ReLU activation function. Because the data labels are scalar values, we used a mean-squared-error loss function for the network. Using a batch size of 256 points, the network was trained for several hours on a machine that holds two NVIDEA Tesla GPUs. We record a copy of the network periodically during training for visualization and debugging purposes.

3. RESULTS

3.1. DNN Training

Figure 4 shows the loss function for the network during each epoch of training. Over this period, the loss tends to decrease in a log-linear fashion. The brief spikes that occur during later epochs are likely due to the batched gradient descent algorithm used to update the network. Using the independent testing dataset, we found that the average error of the network is approximately 0.2 pixels.

Figure 5 includes a series of images that represent the weights of the top-level convolutional neurons in the DAS CNN block. Because they directly interact with the input DAS measurements, they are useful for understanding the structures that the network is looking for in the data.

3.2. DNN Performance

To further explore the behavior of the trained DNN, we calculated the actual/predicted values for each of the models in the testing dataset. Figure 6 shows the distribution of error for each value. These results indicate that 80 to 90 % of the time the network's estimate will be within 1 pixel of the true value. In Figure 7, we plot each of these sets as a point cloud, and calculate error bars within regular bins. These results indicate that the large majority of points are tightly grouped on the expected 1:1 trend-line, and that the prediction error does not vary significantly with the magnitude of the actual parameter. The outliers seen in these charts tend to occur on fibers located near points where the fracture height rapidly changes.

3.3. Hydraulic Fracture Example

To demonstrate the behavior of the DNN, we consider an individual example from the testing dataset (see Figures 8 and 9). The fiber on which recorded DAS measurements was oriented vertically, and was offset 72 and -24 pixels in the x- and y-directions, respectively from the origin of the target fracture. The actual/predicted values for each of the four geometric parameters considered were: H (42/41), H_local (24/24), T (28/28), and T_local (24/23).

Looking at the DAS measurements alone, one might be able to recover the local extent values and the arrival of the fracture tip. By incorporating the known geometric values into the network, the DNN is able to accurately estimate the global extents of the fracture as well.

4. DISCUSSION

The results of our analysis demonstrate the potential for using ML and DNN analysis to monitor the growth of isolated hydraulic fractures in the subsurface. A major benefit of this approach is that the trained DNN can be modified through transfer learning to:

- Incorporate additional data as it becomes available. This could include more complicated numerical simulations or labeled field data.
- Incorporate additional types of measurements in the subsurface (other fiber-optic sensors, geophones, etc.).
- Estimate different parameters in the subsurface (e.g.: fracture aperture).
- Monitor entirely different physical processes (e.g.: geothermal heat flow).

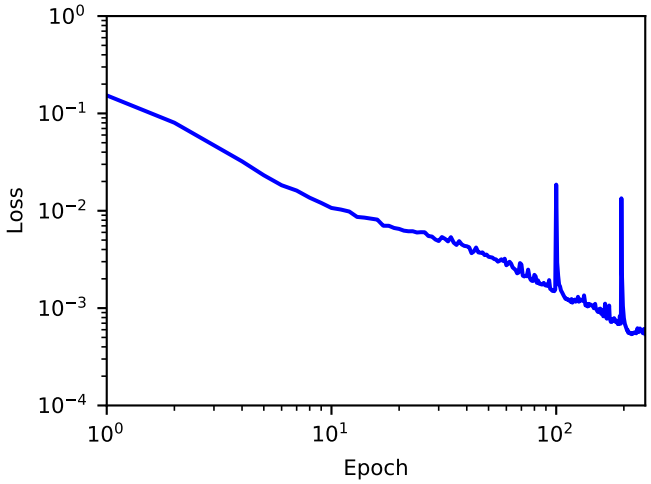

Figure 4: The mean-squared-error loss function for the network during training.

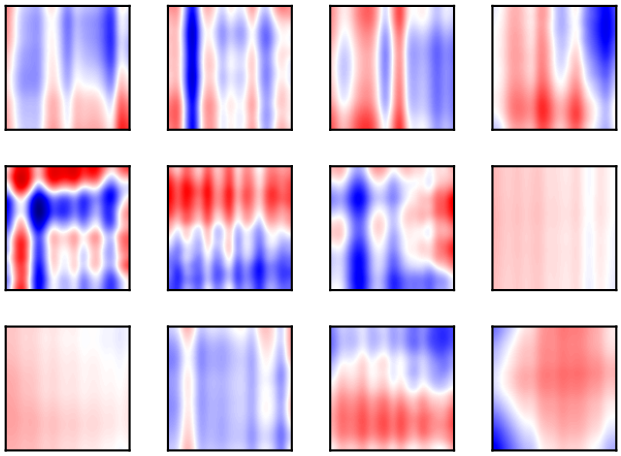

Figure 5: The weights for each of the twelve top-level convolutional neurons.

In our work we tested many different variations of the DNN we developed to process the DAS data. We found that while specific numerical hyper-parameters such as the number of neurons do matter, the type and condition of input data are much more important to the success of the network. Therefore, to make full use of ML approaches, one needs to both understand how the underlying algorithms are implemented and the physics of the underlying system being analyzed.

The above subsection on the hydraulic fracture example demonstrates the importance of a physical understanding of the system. The virtual fiber-optic sensor on which the data was collected is located a point where the local fracture height is about 57% of the global value. We found that when we did not include the sub-block of the network that processes the known geometric information (Geometric NN) that the network had some difficulty in estimating the global fracture height. From the perspective of the physics that govern hydraulic fracturing, we expect that the rates of fracture height and length growth to be balanced. While it is possible to extract the arrival time of the hydraulic fracture from the example DAS, it is not possible to extract the rate of length growth for the fracture. This is a likely explanation for the reduced performance of the limited network, because without this information, it would be difficult for the network to extrapolate back along the fracture and estimate its maximum height.

5. CONCLUSION

In our work, we developed a framework for leveraging machine learning tools to monitor processes within the subsurface, and illustrated why a physical understanding of the system is a key part of this analysis. Moving forward, we will be extending our work to incorporate more complicated physical processes, such as problem of simultaneous fracture growth, and will be experimenting with method to incorporate other physical measurements into the system.

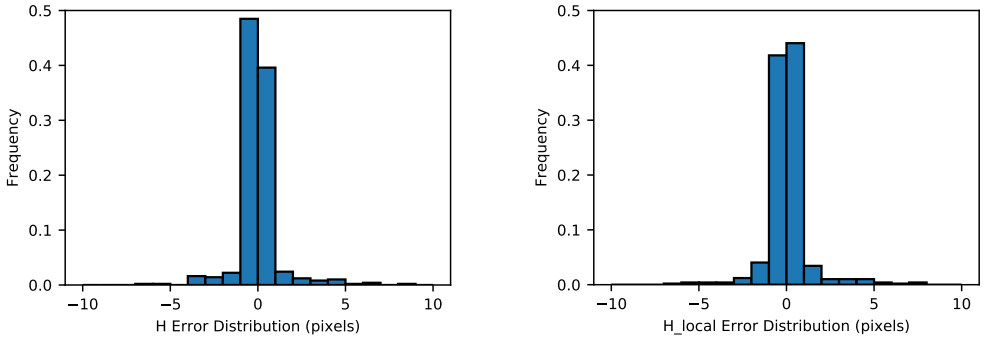

(a) (b)

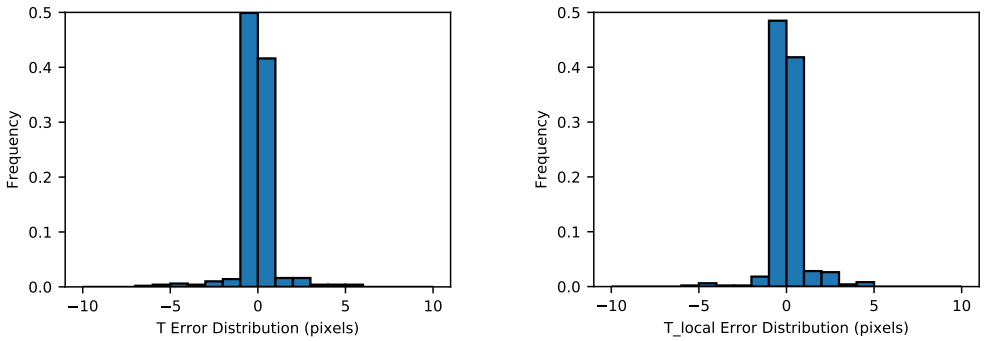

(c) (d)

Figure 6: Histograms showing the error distribution for the features (a) H, (b) H_local, (c) T, and (d) T_local.

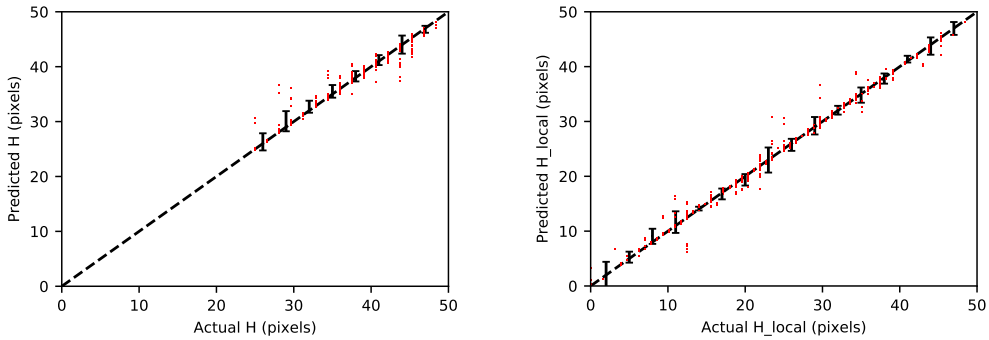

(a) (b)

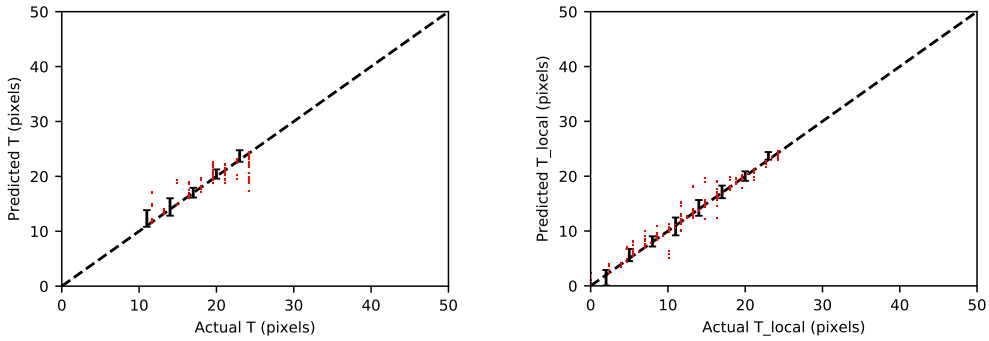

(c) (d)

Figure 7: Comparisons between the actual and predicted values for the features: (a) H, (b) H_local, (c) T, and (d) T_local. Each red dot corresponds to a test case and the black dashed line shows the expected trend.

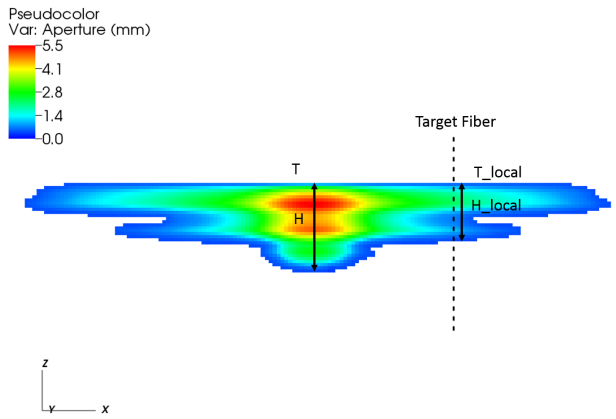

Figure 8: The hydraulic fracture generated during for a network test-case, showing the fracture aperture in color, and the location of the target fiber as a black dashed line.

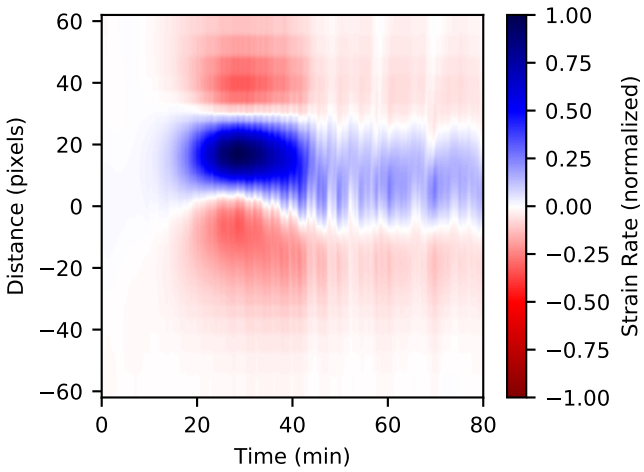

Figure 9: The measured DAS for the target fiber.

6. ACKNOWLEDGMENTS

This work was performed under the auspices of the U.S. Department of Energy by Lawrence Livermore National Laboratory under contract DE-AC52-07NA27344.

REFERENCES

1. Abadi, M., A. Agarwal, P. Barham, E. Brevdo, Z. Chen, C. Citro, and S. Ghemawat. 2015. TensorFlow: Large-scale machine learning on heterogeneous systems.
2. Chollet, F. 2015. Keras documentation.
3. Daley, T. M., B. M. Freifeld, J. Ajo-Franklin, S. Dou, R. Pevzner, V. Shulakova, S. Kashikar, D. E. Miller, J. Goetz, J. Henninges, and S. Luetch. 2013. Field testing of fiber-optic distributed acoustic sensing (DAS) for subsurface seismic monitoring. *The Leading Edge*. 32: 699–706.
4. Hartog, A. H. 2017. An introduction to distributed optical fibre sensors. CRC Press.
5. Hull, R. A., R. Meek, H. Bello, and D. Miller. 2017. Case history of DAS fiber-based microseismic and strain data, monitoring horizontal hydraulic stimulations using various tools to highlight physical deformation processes (Part A). In: *Proceedings of the Unconventional Resources Technology Conference*. SPE.

6. Jin, G., and B. Roy. 2017. Hydraulic-fracture geometry characterization using low-frequency DAS signal. *The Leading Edge*. 36: 975–980.

7. Karrenbach, M., D. Kahn, S. Cole, A. Ridge, K. Boone, J. Rich, K. Silver, and D. Langton. 2017. Hydraulic-fracturing-induced strain and microseismic using in situ distributed fiber-optic sensing. *The Leading Edge*. 36: 837–844.

8. Krizhevsky, A., I. Sutskever, and G. E. Hinton. 2012. Imagenet classification with deep convolutional neural networks. In: *Advances in neural information processing systems*. 1097–1105.

9. Mateeva, A., J. Lopez, H. Potters, J. Mestayer, B. Cox, D. Kiyashchenko, P. Wills, S. Grandi, H. Kees, B. Kuvshinov, W. Berlang, Z. Yang, and R. Detomo. 2014. Distributed acoustic sensing (DAS) for reservoir monitoring with VSP. *Geophysical Prospecting*. 62: 679–692.

10. Settgast, R.R., P. Fu, S. D. C. Walsh, J. A. White, C. Annavarapu, and F. J. Ryerson. 2016. A fully coupled method for massively parallel simulation of hydraulically driven fractures in 3-dimensions. *International Journal for Numerical and Analytical Methods in Geomechanics*. 41: 672–653.

11. Sherman, C., R. Mellors, J. Morris, and F. Ryerson. 2019. Geomechanical modeling of distributed fiber-optic sensor measurements. *Interpretation*. 7: 1–7.